Submitted to Journal of Chemical Physics

LBL-5197
Preprint

SEQUENTIAL IMPULSE MODEL OF DIRECT REACTIONS

Bruce H. Mahan, W. E. W. Ruska, and John S. Winn

July 15, 1976

Prepared for the U. S. Energy Research and Development Administration under Contract W-7405-ENG-48

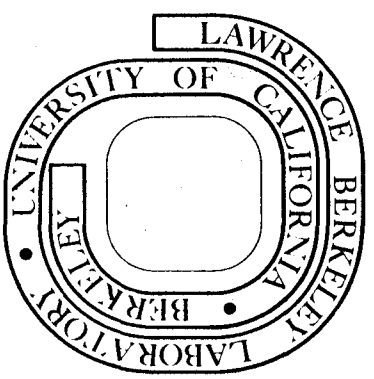

DISCLAIMER

LBL-5197

SEQUENTIAL IMPULSE MODEL OF DIRECT REACTIONS

Bruce H. Mahan, W. E. W. Ruska, and John S. Winn

Department of Chemistry, and Materials and Molecular Research Division of the Lawrence Berkeley Laboratory, University of California, Berkeley, California 94720

ABSTRACT

A model in which the reaction A(BC, C) AB occurs as the result of a sequence of two hard sphere elastic impulses between the A-B and B-C pairs is analyzed. It is shown that the limits of the product velocity vector distribution can be readily obtained from the analytic geometry of the impulse sequence, and that an analytical expression for the detailed product distribution for all mass combinations and energies can be deduced. The results show a propensity for processes in which the velocity of the C atom is changed very little and which therefore lead to products near the spectator stripping velocity. The angular distribution is dependent on, but relatively insensitive to, the ratio of the mutual hard sphere diameter of B and C to their bond distance. The predictions of the model are generally consistent with the features found in the experimental investigations of high energy ion-molecule reactions.

It has proved to be of value to describe the dynamic mechanism of an elementary bimolecular chemical reaction as involving either a short-lived direct interaction of collision partners, or a long-lived collision complex. In the former case, the collision partners are close for a time comparable to a vibrational period, but less than a full rotational period. In the latter case, the partners are close and strongly interacting for several rotational periods. The dividing line between the two classifications is in general somewhat diffuse. Moreover, even when a reaction proceeds predominantly by the long lived complex mechanism, there will be a distribution of lifetimes, and a substantial component of the reactive events may occur by what are effectively direct interactions. Examples of ion-molecule reactions which fall into each extreme classification are now known,[1,2] and reactions which display intermediate behavior have been investigated.[3,4]

Reactions which proceed by direct interaction have product velocity vector distributions which are usually asymmetric about the ±90° axis in the barycentric system. The shape of such a distribution depends on the relative energy at which the reaction is run, the masses of the atoms in the system, and of course on the identity of the reaction itself, since each chemical system has a potential energy surface which is in some or many respects unique. By choosing a trial potential energy surface, then calculating

the results of many classical trajectories generated from a properly weighted set of initial conditions, it is possible to obtain a theoretical product velocity vector distribution which may be compared with experimental results. The effects of various potential energy surface features on the product distributions have been explored in this manner.[5]

Another way to analyze the features of product velocity distributions is to use simplified models of the dynamic processes. It must be recognized that such models may have intrinsic limitations which prevent them from accounting for all features of the product distribution. Nevertheless, they have the virtue of simplicity, and may sometimes stand as rigorous limiting cases which illuminate experimental results even when they do not reproduce them exactly.

A number of simple models for the atom transfer process have been proposed, and at least partially tested against molecular beam scattering data.[6-13] The sequential impulse model proposed by Bates, Cook, and Smith[6] is conceptually simple, and has the capacity for considerable refinement. In this model, the reaction A(BC, C) AB is viewed as an event in which A hits B impulsively and elastically, B then hits C in a like manner, and then A combines with B if their energy of relative motion is less than the dissociation energy of the product molecule. Suplinskas,[8] and George and Suplinskas[9] have elaborated the model, and have shown that it can reproduce the major features of the $Ar^+ - D_2$ reactive scattering.

Gillen, Mahan, and Winn[14] found that a version of the model in which the atoms interact via hard sphere potentials is consistent with the distributions of the products of the reaction of O^+ with D_2 and HD in the regime of high relative energies.

The foregoing applications[8,9,14] involved calculation of the final product velocities from sampled initial conditions by using large digital computers. That is, despite the simplicity of the model, its predictions were obtained by executing trajectory calculations. It would be a valuable aid to the analysis of product distributions if there were a method of finding the collection of trajectories which contribute to the product intensity at any given point in velocity space. It has been pointed out that the sequential impulse model does in fact allow such an "inverted" analysis of the product distribution.[15] Some of the conclusions which can be reached merely by vector analysis have been discussed. In the following sections we review these velocity vector relationships and show how the product intensity distribution can be calculated.

Velocity Vector Analysis

We assume that the atoms A, B, and C interact pairwise only through square well potentials of the same depth. Thus the potential energy surface for the triatomic system is a square trough with a flat bottom and one infinite wall which corresponds to the hard sphere core interaction of the atoms.[16]

The outer wall of the trough has a height equal to the dissociation energy of the reactant BC diatom, or the product AB molecule. This attractive branch of the potential serves only to hold the BC molecule together before reaction, and the AB molecule together after reaction. All significant velocity changes occur as a result of the collisions of the hard sphere cores of the molecules.

To expose the essential features of the model, we shall temporarily assume that the collisions occur such that the three atoms remain in a plane. This assumption will later be eliminated in order to complete the model. An example of a sequence of events which may lead to a reaction is shown in Fig. 1. Initially, the diatom BC (particles 2 and 3, respectively) is stationary in the laboratory, and A (particle 1) moves toward it with a constant velocity $\underset{\sim}{V}_1$. Particles 1 and 2 undergo an impulsive elastic collision, and as a result, their relative velocity vector undergoes a rotation about the center of mass of the A-B system. This means that particle 1 acquires a new laboratory velocity $\underset{\sim}{V}_1'$ which lies somewhere on a circle of radius $V_1B/(A+B)$ whose origin is at the A-B centroid. Here we are letting A, B, and C stand for the masses of the atoms, and using a prime to denote the fact that one impulsive event has occurred. The corresponding laboratory velocity of the B-atom, $\underset{\sim}{V}_2'$, lies somewhere on a circle of radius $V_1A/(A+B)$, which has its origin at the A-B centroid. The magnitude of $\underset{\sim}{V}_2'$ is

$$V_2' = 2 \frac{A}{A+B} V_1 \sin(\frac{\chi_1}{2}) \qquad (1)$$

where χ_1 is the scattering angle in the center of mass of the A-B system. If the full three dimensional case were being considered, both the circles referred to would be spheres.

We now consider particle 2 moving with its constant velocity $\underset{\sim}{V}_2'$ toward particle 3. If the latter is properly positioned, an impulsive elastic collision occurs, particle 2 acquires a new velocity $\underset{\sim}{V}_2''$ and particle 3 assumes the velocity $\underset{\sim}{V}_3''$. In this second impulsive event, the 2-3 relative velocity vector (initially just $\underset{\sim}{V}_2'$) is rotated through an angle χ_2 about the 2-3 centroid. The magnitude of $\underset{\sim}{V}_3''$ is given by

$$V_3'' = 2\left(\frac{B}{B+C}\right) V_2' \sin\left(\frac{\chi_2}{2}\right)$$

$$= 4\left(\frac{A}{A+B}\right)\left(\frac{B}{B+C}\right) V_1 \sin\left(\frac{\chi_1}{2}\right) \sin\left(\frac{\chi_2}{2}\right). \qquad (2)$$

To decide whether or not this sequence of impulses leads to the reaction A(BC, C) AB, we apply a simple criterion: the tip of the velocity vector $\underset{\sim}{V}_3''$ must lie in a stability zone[14] which has limits determined by the requirement that the molecule AB must have an internal (vibrational and rotational) energy which is greater than or equal to zero, and less than its dissociation energy. By energy conservation, these limits can be expressed as values of the translational exoergicity Q, and these are shown for a special case in Fig. 1. It is clear that the direction as well as the magnitude of $\underset{\sim}{V}_3''$ is important to the determination of whether a reaction has occurred.

Having found one sequence of impulses which produce a particular $\underset{\sim}{V}_3''$, we must find all other impulse sequences which lead to the same final result. We note that all possible values of $\underset{\sim}{V}_2'$ lie on a circle of radius $V_1 A/(A+B)$ whose origin is at the 1-2 barycenter. The locus of all possible 2-3 centroid velocities can be found by multiplying all possible values of $\underset{\sim}{V}_2'$ by $B/(B+C)$, and is a circle of radius

$$R = \left(\frac{A}{A+B}\right)\left(\frac{B}{B+C}\right) V_1 \qquad (3)$$

with its center on $\underset{\sim}{V}_1$ at a distance R from the origin. We call this locus the centroid circle.

Because the 2-3 collision is elastic, $\underset{\sim}{V}_3''$ is the base of an isosceles triangle whose other sides are of length $V_2' B/(B+C)$. The perpendicular bisector of $\underset{\sim}{V}_3''$ must pass through the 2-3 centroid, and this centroid must lie on the centroid circle. Thus for the in-plane situation displayed in Fig. 1, there are just two centroids which satisfy both these conditions, and accordingly, there are at most only two in-plane sequences that can lead to a given value of $\underset{\sim}{V}_3''$. One of these sequences corresponds to a large χ_1, and a small χ_2, with the two angles being related by Eq. (2). The other sequence results when the values of χ_1 and χ_2 are interchanged.

Once we recognize that $\underset{\sim}{V}_2'$ need not lie in the plane of $\underset{\sim}{V}_1$ and $\underset{\sim}{V}_3''$, the origin of other sequences which lead to $\underset{\sim}{V}_3''$ becomes clear. When out-of-plane events are considered, the centroid circle becomes a centroid sphere, and the perpendicular bisector of $\underset{\sim}{V}_3''$ becomes a plane. The intersection of this

bisecting plane with the centroid sphere is a "magic circle" perpendicular to the $\underset{\sim}{V}_1 - \underset{\sim}{V}_3''$ plane. As one moves along the magic circle, all the $\chi_1 - \chi_2$ pairs that can lead to scattering at $\underset{\sim}{V}_3''$ are encountered. The extreme values of χ_1 and χ_2 occur when $\underset{\sim}{V}_1$, $\underset{\sim}{V}_2'$, and $\underset{\sim}{V}_3''$ all lie in the same plane.

The foregoing analysis applies to the process A(BC, C) AB, in which A eventually is bound to the atom it strikes first. This "right atom" event is not the only possibility, however. If particle 2 is scattered into the appropriate zone of stability, the molecule AC is formed. If the masses of B and C are equal, this "wrong atom" event is simply related the "right atom" event just discussed. Inspection of Fig. 1 shows that for a given $\underset{\sim}{V}_2'$, the event which would place $\underset{\sim}{V}_2''$ in the stability zone is one in which the scattering angle is the supplement of the angle χ_2 which would have placed $\underset{\sim}{V}_3''$ at the same point in the "right atom" process. The consequence of this is that when the individual events are described by the hard sphere differential scattering cross section, wrong atom reactive processes are just as probable as right atom processes. When the masses of B and C are unequal, this observation is no longer valid, since "right atom" and "wrong atom" process are not described by the same magic circle.

We should also remark that this model does not take into account processes in which A hits B, then C, and then reacts with B. It is difficult to argue on <u>a priori</u> grounds that such processes are unimportant, and their occurrence in real systems may lead to failures of the model. On the other hand,

George and Suplinskas[9] found these collision sequences to be relatively unimportant in their trajectory analysis of the kinematic reaction model for the $Ar^+(D_2, D)\ ArD^+$ reaction. For this and similar mass combinations, this collision sequence will place the product velocity very close to the locus predicted by the elastic spectator model. In the high energy regime, where spectator or elastic spectator process do not lead to stable products, the A hits B, A hits C, A reacts with B sequence will certainly not be important.

A number of useful conclusions can be drawn directly from Fig. 1. First, there will be certain $\underset{\sim}{V}_3''$ vectors for which the perpendicular bisector does not intersect the centroid sphere. Even though these values of $\underset{\sim}{V}_3''$ might be consistent with the total energy and momentum conservation laws, they can not be produced by a sequence of two elastic impulses. For example, events in which $\underset{\sim}{V}_3''$ is directed at 180° in the laboratory coordinate system can not occur. Thus there is no exactly backward recoil of particle C, and no exactly forward recoil of the AB product. This observation is of interest in connection with deviations from the ideal spectator stripping phenomenon.[12,17] Forward recoil could occur if, prior to the A-B impulse, the vector $\underset{\sim}{V}_1$ were increased in magnitude with the center of mass velocity of the total system held constant. This could occur if there were an attractive potential between reactants, and this is in fact the mechanism for forward recoil proposed in the so-called modified stripping model.[12]

One can also see that forward recoil could occur if, during the B-C collision, the B-C relative velocity vector were increased in length, so that this collision would appear to be super-elastic. This could occur in a real system if there were a repulsive energy release between B and C as the products separated. This is the basic idea involved in the so-called direct interaction with product repulsion (DIPR) model[10,13] for reaction dynamics. The velocity vector analysis connected with the sequential impulse model clearly shows that more than one property of a potential energy surface can produce a given feature of the product velocity distribution.

It is clear that $\underset{\sim}{V}_3''$ vectors directed at angles other than 180° are accessible only if the magnitude of $\underset{\sim}{V}_3''$ is small enough so that there is an intersection of the bisecting plane and the centroid sphere. If we consider the in-plane scattering sequence we find from Fig. 1 that the angles ξ_+ and ξ_- between $\underset{\sim}{V}_1$ and the two values of $\underset{\sim}{V}_2'$ which are defined by the intersection of the centroid circle and the bisector of $\underset{\sim}{V}_3'$ are given by

$$\cos^2\xi_{\pm} = \frac{1}{2}(\sin^2\varepsilon + \frac{V_3''}{2R}\cos\varepsilon) \pm \frac{1}{2}[(\sin^2\varepsilon + \frac{V_3''}{2R}\cos\varepsilon)^2 - 4(\frac{V_3''^2}{4R})]^{1/2} . \quad (4)$$

The corresponding values of χ_2 are given by

$$\cos^2(\frac{\chi_2}{2})_{\pm} = 1-(V_3''/4R\cos\xi_{\pm})^2. \quad (5)$$

The situation in which the discriminant of Eq. (4) is zero corresponds to the bisector being tangent to the centroid circle.

For a given laboratory scattering angle ε for particle 3, this corresponds to the greatest magnitude of V_3'' which can be produced by an elastic impulse sequence. Setting the discriminant equal to zero, we find

$$(V_3'')_{max} = 2R(\cos\varepsilon+1). \qquad (6)$$

Thus the limiting values of $\underset{\sim}{V}_3''$ describe a cardioid which has a cusp at the origin of laboratory coordinate system.

There is a corresponding cardioid which gives the maximum velocity of the AB product in the center of mass system, and this is illustrated in Fig. 2. It is of interest to note that AB product at the cusp of the cardioid is moving with the spectator stripping velocity. One very simple picture of product velocity distributions is provided by the elastic spectator model, in which the product speed relative to the center of mass is expected to be at all angles equal to the spectator stripping velocity. Such a distribution would occur if the AB product were formed by the spectator stripping process, and then rebounded elastically as a unit from the C atom. Observed deviations from this elastic spectator model are then to be attributed to inelasticity or superelasticity of the collision of AB with C. The reflection-spectator[12] and DIPR models[10] are variations of this elastic spectator model theme. The limiting cardioid derived for the sequential impulse model shows that apparently superelastic deviations from the elastic spectator model can occur quite naturally

without the intervention of special types of reactant attraction or product repulsion.

The accessible part of the product stability zone is bounded on the outside by the limiting cardioid, and on the inside by a circle whose radius is determined by Q_{min}, the smallest value of the translational exergicity which can lead to a stable AB product. The size of the limiting cardioid is proportional to R, and thus scales with the initial velocity V_1. The size of the inner stability circle is determined by subtracting a fixed quantity (the AB dissociation energy) from the initial relative energy, and taking the square root of the result. Thus the size of the Q_{min} circle does not scale with V_1. The size of the kinematically accessible zone can be described at all energies by one cardioid, if the units of the diagram are changed as the energy changes. However, as the initial energy is increased, on such a diagram, the radius of the inner stability circle increases and the size of the stability zone decreases. This is shown in Fig. 2 by several inner stability circles which correspond to different initial relative energies.

As the initial relative energy increases, the inner stability circle expands and eventually intersects the limiting cardioid at the cusp. This situation corresponds to the critical energy at which the spectator stripping peak which is prominent in many product distributions is expected to be lost. In most ion-molecule reactions which have been investigated, the product scattered in the direction of the

initial projectile is in fact retained, but moves to speeds which are greater than the spectator stripping value, and which lie the stability zone. As indicated above, the cause of this forward recoil is to be found in features that are not included in the strict hard sphere sequential impulse model. We note that all reactions which exhibit forward recoil[17-19] at high energies are substantially exoergic, and those that do not show forward recoil[14,20] are thermoneutral or weakly exoergic. This suggests that exoergicity is the factor which promotes forward recoil. It is in general an open question as to whether this forward recoil comes from reactant attraction or product repulsion. Experimentation with velocity vector diagrams of the type of Fig. 1 suggests that product repulsion is the most efficient way in which reaction exoergicity can be used to stabilize the reaction product. In the so-called modified stripping model,[12,21] it is proposed that the small difference of the polarization attraction between the reactants and products accounts for the minuscule deviations of the product intensity peak from the spectator stripping velocity which are observed for ion-molecule reactions at very low energy. In view of the other possible mechanisms of forward recoil, this proposal seems very speculative.

In the strict sequential impulse model, the potential surface represents the possible interaction of hard spheres, and there is no mechanism for exactly forward recoil of the AB product. Thus the product distribution assumes a crescent

shape when the initial energy is high enough to make spectator stripping impossible. As the energy is increased still further, the inner stability circle makes a second intersection with the limiting cardioid at 180°. Thus according to the sequential impulse model it is the rebound scattering which is lost after the stripping contribution has disappeared. It should be noted that for many mass combinations, the predictions of the sequential impulse model will fail in the large angle region, because this region may be populated by product which is formed by multiple or "chattering" collisions[16] in which B rebounds between A and C several times. This accounts, at least partially, for the observations[14,20] of product in the large angle region at very high energies.

It is of interest to examine the type of impulse sequence which leads to AB product with no internal excitation. For the thermoneutral potential surfaces we are treating, this corresponds to a translational exoergicity Q equal to zero. More significantly, it corresponds to impulse sequences which produce equal velocities for A and B. A sphere in velocity space can be drawn with its origin at the center of mass velocity of the ABC system, and its radius equal to the AB speed which corresponds to Q = 0. A second sphere which is the locus of all possible velocities of A after the A-B collision can also be drawn with radius V_1 B/(A+B), centered on $\underset{\sim}{V}_1$ A/(A+B). Since the velocity of A in all sequences is completely determined by the result of the first impulse, and since in a Q = 0 event A and B and their mutual center

of mass must have velocities on the Q = 0 sphere, the only double impulse sequences which can produce unexcited products lie on the intersection (if any) of the Q = 0 sphere and the $\underset{\sim}{V}_1'$ sphere. The intersection of the spheres produces a circle whose plane is perpendicular to $\underset{\sim}{V}_1$. After working out the analytic geometry, we find that according to the sequential impulse model, scattering to give unexcited AB product occurs only at a barycentric angle θ_o given by

$$\cos\theta_o = \frac{ABCM+2A^2C^2-B^2M^2}{2AC[AC(A+B)(B+C)]^{1/2}} \qquad (7)$$

if it occurs at all. We note also that the C product will appear at the supplement to this angle which is also a point of tangency between the limiting cardioid and the Q = 0 circle for the C product. This must be true, since the limiting cardioid is the highest velocity allowed by the sequential impulse model, and Q = 0 corresponds to the highest relative velocity allowed by any model.

Since the limiting cardioid and the Q = 0 circle are tangent only at the barycentric given by Eq. (7), it is at this angle that the accessible part of the stability zone is widest. For the $N^+ - H_2$ system this angle is 51°, and for $O^+ - H_2$ it is 47°. It is also useful to realize that as the initial projectile velocity increases toward infinity, the Q = 0 circle and the limiting cardioid scale together and maintain their tangency. However, the inner stability circle intercepts greater and greater fractions of the limiting

cardioid as the energy increases, as Fig. 2 indicates. As the limit of infinite relative velocity, is approached, the accessible part of the stability zone contracts to the point on the cardioid at θ_o. It is this contraction that is responsible for the product intensity lobes observed[14,20] in the vicinity of θ_o in the $N^+ - H_2$ and $O^+ - H_2$ systems at high relative energies.

We have discussed the events in which an A-B collision is followed by a B-C collision. In order for this sequence to occur, the angle α between the intermediate velocity $\underset{\sim}{V}_2'$ and the BC bond axis must be less than $\pi/2$. For $\alpha > \pi/2$, the motion of B most often will tend to carry it away from C, and there will be no B-C collision possible. If the AB product in such events is stable, it will appear at the spectator stripping velocity. Stripping is also possible for values of α somewhat smaller than $\pi/2$ if the mutual hard sphere diameter of the B-C pair is less than the impact parameter for the second collision. Thus, for this hard sphere potential surface, over half of the total reactive events can appear at the spectator stripping velocity.

These observations make it clear how spectator stripping can be so prominent in the product velocity vector distributions of ion-molecule reactions. We note that in real systems, the potential energy surfaces must have only a weak dependence on the ABC angle if they are to produce distributions which are comparable to those derived from the hard sphere model.

Such behavior will be facilitated if there is a strong long range attraction between A and B in the product channel, as there is when A is an alkali atom and B is a halogen. However, if the potential surface is angle independent, stripping is possible even when A and B collide essentially head-on. Thus if spectator stripping is described as involving grazing collisions, it is the B-C interaction, and not necessarily the A-B interaction which must be of the grazing type.

Product Intensity Distributions

To formulate the product intensity distribution, we note first that the total rate at which A-B collisions occur is

$$\mathcal{R} = \sigma_{12}(n_1)(n_{23})\ V_1 \qquad (8)$$

where σ_{12} is the total cross section for A-B collisions, and n_1 and n_{23} are the concentrations of projectile and target molecules respectively. These collisions produce various values of $\underset{\sim}{V}_2'$ which terminate on a sphere in velocity space. The corresponding centroids of the 2-3 system all lie on the centroid sphere. In a polar coordinate system centered at R, the origin of the centroid sphere, the distribution of 2-3 centroids is uniform. Therefore, the probability that the centroid velocity will lie in θ, $\theta+d\theta$, ϕ, $\phi+d\phi$ is

$$d^2P_1 = \frac{1}{4\pi} \sin\theta d\theta d\phi. \qquad (9)$$

It is convenient to take the polar axis of this system parallel to $\underset{\sim}{V}_3''$.

Now we find the probability that a 2-3 collision will occur in which the scattering angle is χ_2. For a specified $\underset{\sim}{V}_2'$, the scattering angle χ_2 will depend on the orientation of the B-C bond axis with respect to $\underset{\sim}{V}_2'$. According to Fig. 3, the probability of a orientation expressed by the angles α and γ is

$$d^2P_2 = \frac{1}{4\pi} \sin\alpha d\alpha d\gamma.$$

Since $\sin\alpha = b/r_o$, where b is the impact parameter and r_o is the equilibrium 2-3 bond distance, we can write

$$d^2P_2 = \frac{1}{4\pi r_o^2} \frac{bdbd\gamma}{(1-\frac{b^2}{r_o^2})^{1/2}} \qquad (10)$$

By making use of the relation

$$bdbd\gamma = I_{23}\, d^2\omega_{23} \qquad (11)$$

where I_{23} is the differential scattering cross section for the second impulse, and $d^2\omega_{23}$ is the differential solid angle in the 2-3 barycentric system, we can deduce the expression

$$d^2P_2 = \frac{I_{23}d^2\omega_{23}}{4\pi r_o^2(1-b^2/r_o^2)^{1/2}}.$$

Thus, the differential rate for collisions in which the 2-3 centroid is in $d\theta$, $d\phi$ and the 2-3 scattering is in $d^2\omega_{23}$ is

$$d^4\mathcal{R} = (n_1)(n_{23})\ V_1\ \sigma_{12}\ d^2P_1\ d^2P_2$$

$$d^4\mathcal{R} = (n_1)(n_{23})\ V_1\ \sigma_{12}\ \frac{I_{23}d^2\omega_{23}\sin\theta d\theta d\phi}{16\pi^2 r_o^2(1-b^2/r_o^2)^{1/2}}. \qquad (12)$$

It is now necessary to eliminate the differential solid angle element $d^2\omega_{23}$ in favor of $d^2\Omega_3$, the solid angle element for particle 3 in the laboratory coordinate system. The necessary relation is

$$\frac{d^2\Omega_3}{d^2\omega_{23}} = \frac{u_3^2}{V_3^2}\sin(\frac{\chi_2}{2})$$

where u_3 is the speed of particle 3 in the 2-3 barycentric system, and we have discontinued the prime notation. Since

$$V_3 = 2u_3 \sin\frac{\chi_2}{2}$$

we have

$$d^2\omega_3 = 4\sin(\frac{\chi_2}{2})\ d^2\Omega_3. \qquad (13)$$

In addition, we wish to eliminate $d\theta$ in favor of dV_3. From Fig. 4 we see that

$$V_3/2R - \cos\varepsilon = \cos\theta. \qquad (14)$$

Therefore

$$dV_3/2R = -\sin\theta d\theta.$$

We take the absolute value of this expression and substitute it,

together with Eq. (13) in Eq. (12) and obtain

$$d^4\mathcal{R} = (n_1)(n_{23})\, V_1 \frac{\sigma_{12} I_{23}}{8\pi^2 r_o^2 V_3^2 \mathcal{R}} V_3^2\, dV_3\, d^2\Omega_3 \frac{\sin(\frac{\chi_2}{2})d\phi}{(1-b^2/r_o^2)^{1/2}}. \quad (15)$$

To obtain the total rate of collisions which produce V_3 in $(V_3)^2\, dV_3\, d^2\Omega_3$ it is only necessary to integrate Eq. (15) over the magic circle. If we introduce the relations

$$I_{23} = d_{23}^2/4$$

$$b^2 = d_{23}^2 \cos^2(\frac{\chi_2}{2})$$

which hold for hard sphere scattering, integrate over ϕ and rearrange, we find

$$\frac{1}{(n_1)(n_{23})V_1} \frac{d^3R}{d^3V_3} = \frac{\sigma_{12} d_{23}^2}{32\pi^2 r_o^2 V_3^2 R} \int_o^{2\pi} \frac{\sin\frac{\chi_2}{2}\, d\phi}{(1-\frac{d_{23}^2}{r_o^2}\cos^2\frac{\chi_2}{2})^{1/2}}. \quad (16)$$

The quantity on the left is the rate of product formation per unit projectile flux, per target gas molecule, per unit velocity space volume. It is, therefore, equal to the specific intensity $\bar{I}$ which is reported in maps of product velocity vector distributions.[18]

We note that the total intensity of a process other than spectator stripping is proportional to the factor $\sigma_{12}(d_{23}^2/r_o^2)$, which is the cross section for the first impulse times the chance that the second impulse will occur. The factor of V_3^{-2}

tends to promote a high product intensity near the spectator stripping velocity, and this is modified by the value of the integral over the magic circle.

In order to perform the integration over the magic circle, the relation between ϕ and the scattering angle χ must be found. However, in the special case that $d_{23} = r_o$, this relation is unnecessary, and Eq. (16) immediately reduces to

$$\bar{I} = \frac{d_{12}^2}{16 V_3^{\,2} R} \tag{17}$$

where we have used $\sigma_{12} = \pi d_{12}^2$. In this special case, all 1-2 impulses lead to 2-3 impulses if $\alpha < \pi/2$. The intensity distribution is controlled only by the factor of V_3^{-2} and the stability limits. To recover the total cross section for all processes in which two impulses occur, we execute

$$\sigma = \iiint \bar{I} V_3^{\,2} \, dV_3 \, d^2\Omega = \frac{1}{16} \frac{d_{12}^2}{R} \iiint dV_3 \, d^2\Omega \tag{18}$$

where the integration includes everything inside the limiting cardioid. Therefore

$$\sigma = \frac{\pi}{4} \frac{d_{12}^2}{R} \int_o^{\pi} R(1+\cos\varepsilon) \sin\varepsilon d\varepsilon$$

$$= \frac{\pi}{2} d_{12}^2 \tag{19}$$

which is half of the cross section for 1-2 collisions. The missing fraction of σ_{12} corresponds to collisions in which the second impulse does not occur, since $\alpha > \pi/2$. The

contribution from such collisions appears exactly at the spectator stripping velocity. To obtain the total cross section for reaction only, one must integrate over the region between the inner product stability circle and the limiting cardioid. A particularly simple case occurs at the critical energy above which spectator stripping leads to product instability. At this energy, the stability circle for particle 3 has a radius of, and is centered at, $\underset{\sim}{V}_1$ A/M, where M is the total mass. Therefore

$$(V_3)_{min} = 2V_1(A/M)\cos\varepsilon \tag{20}$$

with $0 \leq \varepsilon \leq \pi/2$. If the masses are such that the only intersection of the cardioid and the circle is at $V_3 = 0$, the total reaction cross section at this critical energy is

$$\sigma = \frac{\pi}{8}\frac{d_{12}^2}{R}\left[\int_o^{\pi}(V_3)_{max}\sin\varepsilon d\varepsilon - \int_o^{\pi/2}(V_3)_{min}\sin\varepsilon d\varepsilon\right]$$

$$= \frac{\pi}{2}d_{12}^2\left[1 - \frac{(A+B)(B+C)}{4BM}\right]. \tag{21}$$

As the initial energy increases still more, the size of the accessible stability zone continues to decrease. In the limit of infinite initial relative energy, the stability circle and the limiting cardioid are tangent at one point, and the reaction cross section is zero. It must be stressed that Eq. (21) is valid only at one energy, and only for mass combinations for which the stability circle intersects the

cardioid only at the cusp. For higher energies, there will be two intersections, and for certain mass combinations (A > B < C) the stability circle may intersect the cardioid first at its extremum, and not at its cusp. It is, of course, still possible to calculate total reaction cross sections for these situations, but the geometry of the limiting cardioid and stability circle must be examined carefully in order to determine the proper domain of integration.

In order to obtain the intensity distribution by integration of Eq. (16), a relation between χ_2 and the angle ϕ must be found. The basic expression, derived from the geometry of the magic circle and the 2-3 elastic scattering triangle shown in Fig. 4 is

$$\cot^2\left(\frac{\chi_2}{2}\right) = \left(\frac{2s}{V_3}\right)^2 = (\ell^2+\rho^2-2\ell\rho\cos\phi)(2/V_3)^2 \qquad (22)$$

Here ρ is the radius of the magic circle, and ℓ is the perpendicular distance of its center from the vector $\underset{\sim}{V}_3$. By introducing the quantity

$$\eta = 1 - \frac{d_{23}^2}{r_o^2} \qquad (23)$$

the integral in Eq. (16) can be written

$$\mathcal{I} = \int_o^{2\pi} \frac{d\phi}{\left(1+\eta\,\mathrm{ctn}^2\left(\frac{\chi_2}{2}\right)\right)^{1/2}} . \qquad (24)$$

Substitution of Eq. (22) leads to

$$\mathcal{I} = 2\int_0^{\pi} \frac{d\phi}{(a-b\cos\phi)^{1/2}} \tag{25}$$

with

$$a = 1 + 4\eta(\ell^2+\rho^2)/V_3^2 \tag{26}$$

and

$$b = 8\eta\ell\rho/V_3^2. \tag{27}$$

The integral is known,[22] and can be written

$$\mathcal{I} = \frac{4}{(a+b)^{1/2}} F\left(\frac{\pi}{2}, \frac{2b}{a+b}\right) \tag{28}$$

where $F(\frac{\pi}{2}, m)$ is the complete elliptic integral of the first kind. The specific intensity of the C product in velocity space is therefore

$$\bar{I}_c = \frac{\sigma_{12}(1-\eta)F(\frac{\pi}{2}, \frac{2b}{a+b})}{8\pi^2 V_3^2 R(a+b)^{1/2}} . \tag{29}$$

Thus, once the sizes of the particles have been specified, the intensity distribution can be obtained readily with the aid of standard tables of the elliptic integral.

The intensity distribution function for particle C was evaluated at points on a rectangular grid, and then lines of constant intensity were drawn using a visual interpolation procedure. The results for two values of d_{23}/r_o are plotted in Fig. 5. While some accuracy is lost by using a finite size

grid, this procedure to some degree mimics the loss of resolution imposed by any real experimental apparatus or by the bin size in a trajectory calculation. The distribution of particle C is, of course, equivalent to that of the molecule AB, and is a somewhat more convenient representation of the reaction dynamics, for reasons which will become evident in the subsequent discussion.

For values of V_3 which are well inside the limiting cardioid, the intensity contours in Fig. 5 are very nearly circular, and have values which fall off almost exactly as V_3^{-2}. The reason for this is that the elliptic integral in Eq. (29) is a slowly varying function of V_3 and ϵ, except at very small values of V_3. Thus the intensity distribution is controlled principally by the limiting cardioid, the factor of V_3^{-2}, and any inner stability circle determined by the dissociation energy of the AB product. Figure 5 shows that the distribution is relatively insensitive to the value of the mutual hard sphere diameter chosen for particles 2 and 3. As d_{23} is made smaller, the total intensity associated with the double impulse sequence becomes smaller, and is more sharply peaked near $V_3 = 0$.

The masses of the atoms appear in Eq. (29) only through the factor R. Thus Fig. 5 can be made to represent the product distribution for any mass combination merely by placing the projectile velocity and center of mass velocity properly with respect to the vector R. When C > B, the cardioid and centroid sphere tend to be small compared with V_1, particle

C will tend to be concentrated near zero velocity in the laboratory, and AB will be forward scattered. When C < B, the centroid sphere and limiting cardioid are large, and AB tends to appear at larger center of mass scattering angles. When B = C << A, product velocity vector distributions will be very insensitive to isotopic mass variations. The reactions of N_2^+, O_2^+, C^+, N^+, and O^+ with H_2, D_2 and HD have displayed isotope effects of these kinds in the high relative energy, direct interaction regime.

As a check of the validity of the analytical treatment of the sequential impulse model we evaluated the product velocity vector distribution by carrying out classical trajectory calculations for the hard sphere model. The radii of the spheres were taken to be 0.48 Å for the projectile A, and 0.25 Å for B and C, which correspond to values intermediate between the extremes used in Fig. 5. The diatom was initial stationary with a bond distance of 0.75 Å. From a properly weighted set of initial orientations and impact parameters, trajectories were calculated, and the number terminating in various bins in velocity space were counted. In order to make maximum use of the trajectories, an azimuthal integration was performed by collecting all events in which V_3 and the angle ε had fixed values in one bin which was then weighted with a factor of $(V_3 \sin\varepsilon)^{-1}$.

The resulting distribution was plotted as the contour map shown in Fig. 6. The lower half of the map shows the bin size and the weighted amplitudes collected in each bin.

Approximately six thousand trajectories were used to construct the map. When allowance is made for statistical fluctuations and the bin size, the resemblance of Fig. 6 to Fig. 5 is very close. Other sets of trajectory calculations were run, and found to be consistent with the major results of the analytical sequential impulse model: the laboratory distribution of particle C was insensitive to variation of the masses and mutual radii of the particles. It is obvious, but still worth stressing, that the analytical treatment revealed these properties much more clearly than could any finite set of trajectory calculations.

A few remarks are in order concerning "wrong atom" or knock-out processes in which A hits B, but reacts with C. As we have noted, when the masses of B and C are equal, the velocity vector distribution for AC formed by the wrong atom process is identical to that of AB formed by the right atom process. This is not true if B and C have unequal masses. The magic circle for wrong atom processes proves to be given by the intersection of the centroid sphere with a second sphere of radius $|\gamma V_2'' (1-\gamma^2)|$, which is centered at $V_2''/(1-\gamma^2)$, where γ is the mass ratio C/B. When γ is unity, this second sphere attains an infinite radius, and becomes the bisecting plane discussed above. The limiting cardioid for the wrong atom process is given by

$$(V_2'')_{max} = 2R(\cos\varepsilon+\gamma)$$

which reduces to an expression equivalent to Eq. (6) when the masses of B and C are equal. From the limiting cardioid alone it is possible to deduce certain general characteristics of the product distribution for wrong atom reactions. These prove to be qualitatively consistent with the results of trajectory calculations in which the wrong atom processes are identified. However, these characteristics are inconsistent with experimentally determined product distributions for the O^+-HD and N^+-HD systems. Apparently, wrong atom processes are not important in real systems. Consequently, we have not pursued the significantly more complicated problem of an analytical treatment of wrong atom processes.

Summary

The analytical treatment of the sequential impulse model for the reaction A(BC, C) AB has been carried out under the assumption that the atoms interact as hard spheres. The results show a strong propensity for processes in which the velocity of C is changed very little, and which therefore lead to products near the spectator stripping velocity. The angular distribution of products is relatively insensitive to the mutual hard sphere diameters of the atoms B and C, particularly in the large angle scattering region. The effects of isotopic variations can be predicted rather simply by using one map of the C product distribution. The predictions of the model are generally consistent with several features found in the experimental investigations of high energy ion-molecule reactions.

Acknowledgement

This work was done with support from the U. S. Energy Research and Development Administration.

References

1. W. Koski in Advances in Chemical Physics, vol. XXX, edited by K. P. Lawley (Wiley and Sons, New York, 1975) pp. 185-246.
2. B. H. Mahan in MTP International Review of Science, Series II, vol. 9., edited by D. R. Herschbach (Butterworth and Co., London 1976).
3. M. H. Chiang, E. A. Gislason, B. H. Mahan, C. W. Tsao, and A. S. Werner, J. Phys. Chem. 75, 1426 (1971).
4. B. H. Mahan and T. M. Sloane, J. Chem. Phys. 59, 5661 (1973).
5. See, for example, J. D. McDonald, J. Chem. Phys. 60, 2040 (1974).
6. D. R. Bates, C. J. Cook, and F. J. Smith, Proc. Phys. Soc. (London) 83, 49 (1964).
7. J. C. Light and J. Horrocks, Proc. Phys. Soc. (London) 84, 527 (1964).
8. R. J. Suplinskas, J. Chem. Phys. 49, 5046 (1968).
9. T. F. George and R. J. Suplinskas, J. Chem. Phys. 54, 1037 (1971).
10. P. J. Kuntz, Trans. Faraday Soc. 66, 2980 (1970).
11. D. T. Chang and J. C. Light, J. Chem. Phys. 52, 5687 (1970).
12. P. M. Hierl, Z. Herman, and R. Wolfgang, J. Chem. Phys. 53, 660 (1970).
13. M. Marron, J. Chem. Phys. 58, 153 (1973).
14. K. T. Gillen, B. H. Mahan, and J. S. Winn, J. Chem. Phys. 59, 6380 (1973).

15. B. H. Mahan in Interactions Between Ions and Molecules, edited by P. Ausloos (Plenum, New York, 1974).

16. B. H. Mahan, J. Chem. Ed. 51, 308, 377 (1974).

17. M. Chiang, E. A. Gislason, B. H. Mahan, C. W. Tsao, and A. S. Werner, J. Chem. Phys. 52, 2698 (1970).

18. W. R. Gentry, E. A. Gislason, B. H. Mahan, and C. W. Tsao, J. Chem. Phys. 49, 3058 (1968).

19. K. Lacmann and A. Henglein, Ber. Bunsenges. Physik. Chem. 69, 292 (1965).

20. B. H. Mahan and W. E. W. Ruska, to be published.

21. Z. Herman, J. Kerstetter, T. Rose, and R. Wolfgang, Disc. Faraday. Soc. 44, 123 (1967).

22. P. F. Byrd and M. D. Friedman, Handbook of Elliptic Integrals for Engineers and Physicists, Springer, Berlin, 1954.

Figure Captions

Fig. 1. A velocity vector diagram for the sequential impulse model. The two values of $\underset{\sim}{V}_2'$ represent the two possible in plane scattering sequences which can lead to the final product state $\underset{\sim}{V}_3''$. The Q circles represent the zone in which $\underset{\sim}{V}_3''$ must lie in order for a stable AB product to be formed.

Fig. 2. The limiting cardioid for NH^+ from the $N^+(H_2,H)NH^+$ reaction. The spectator stripping velocity lies at the cusp of the cardioid. The circles represent the low velocity limit for product stability at three the initial relative energies E_r = 6.9 eV, 12.5 eV, and infinity.

Fig. 3. The geometry of a sequential impulse collision. The BC bond axis makes an angle α with the velocity vector $\underset{\sim}{V}_2'$, and the impact parameter for the second collision is b.

Fig. 4. The geometry of the (a) centroid sphere and (b) magic circle.

Fig. 5. A contour map of the specific intensity of the C product atom according to the sequential impulse model for two values of the parameter d_{23}/r_o. Note that the contribution of the spectator stripping events, which would appear at the cusp, is not included.

Fig. 6. A contour map of the specific intensity of the C atom product according to the trajectory method. The lower half of the map shows the relative amplitudes of products and the bin size, which is approximately four times the area of the grid size used to plot Fig. 5.

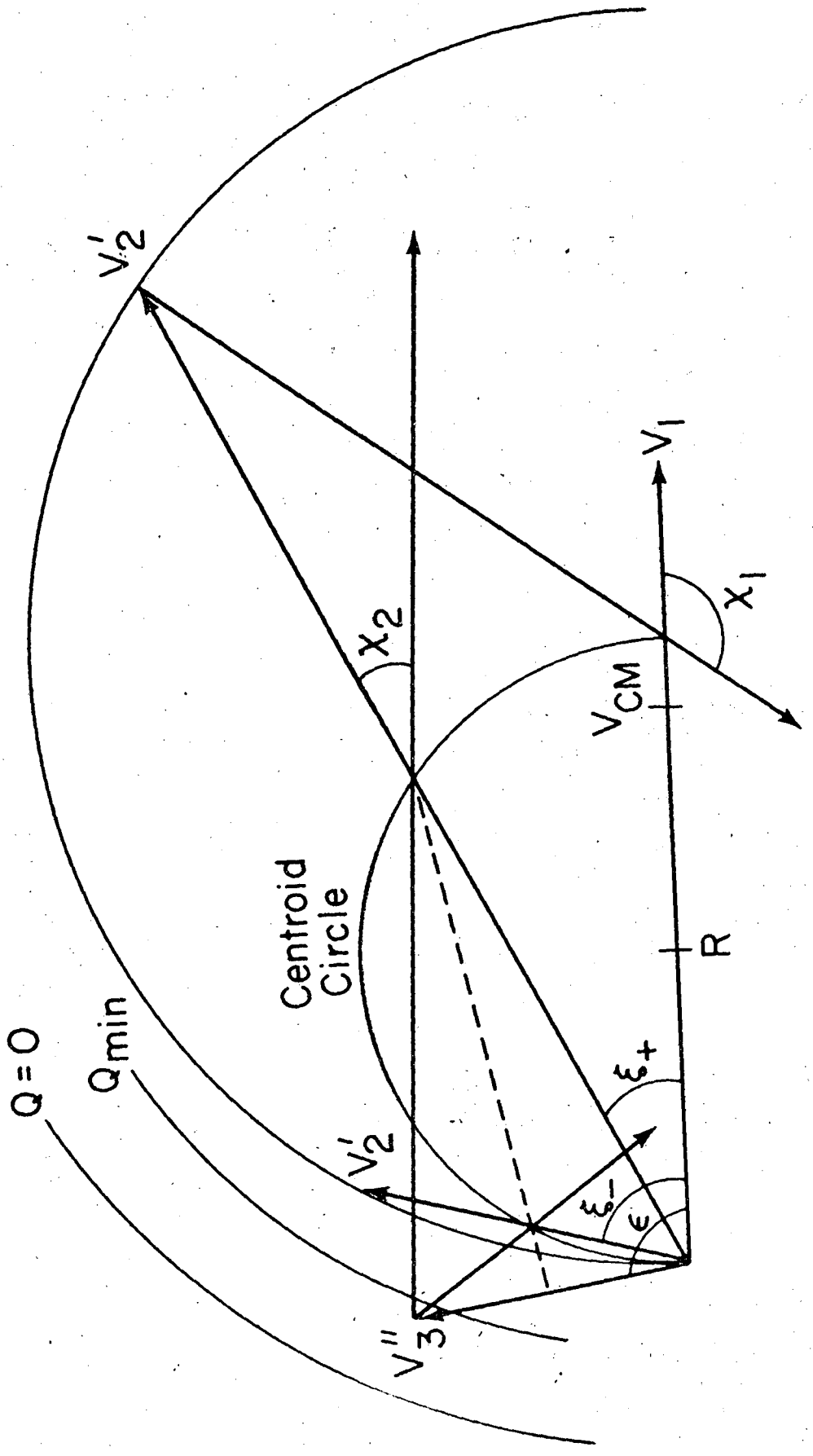

Fig. 1

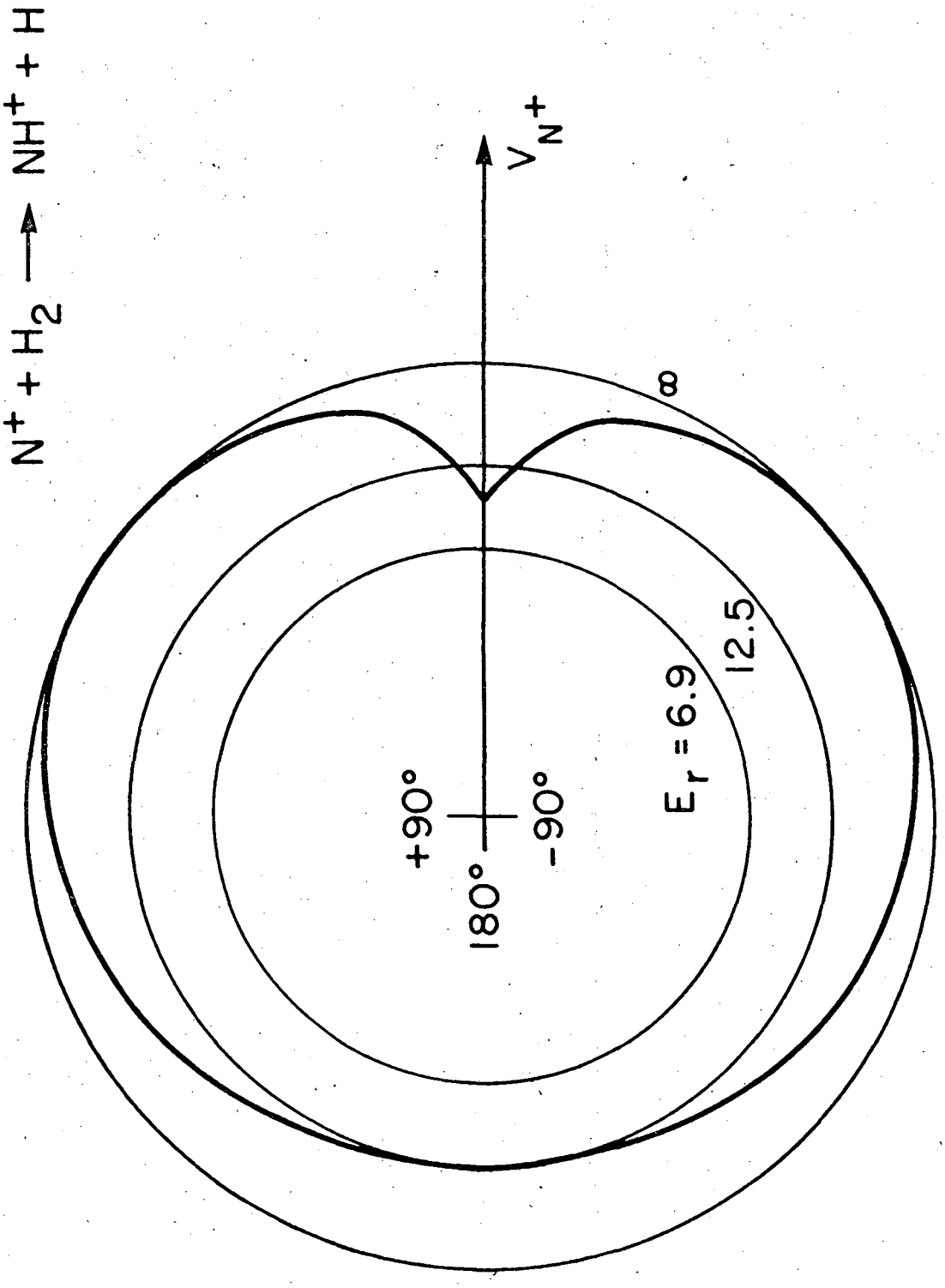

Fig. 2

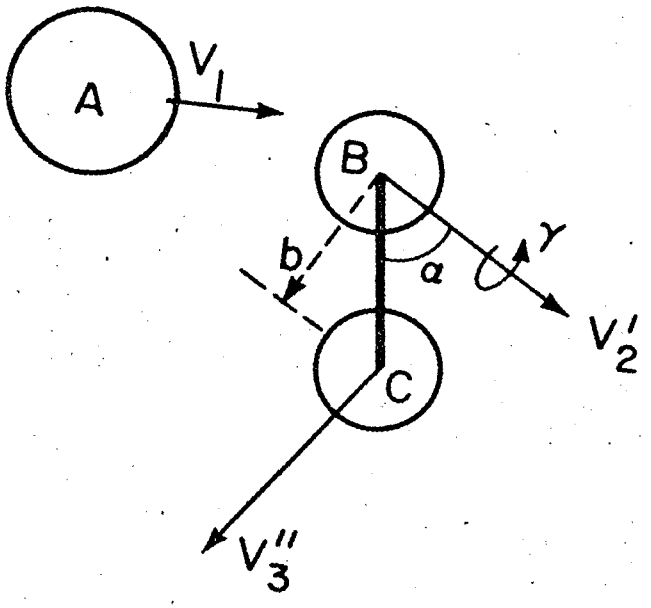

Fig. 3

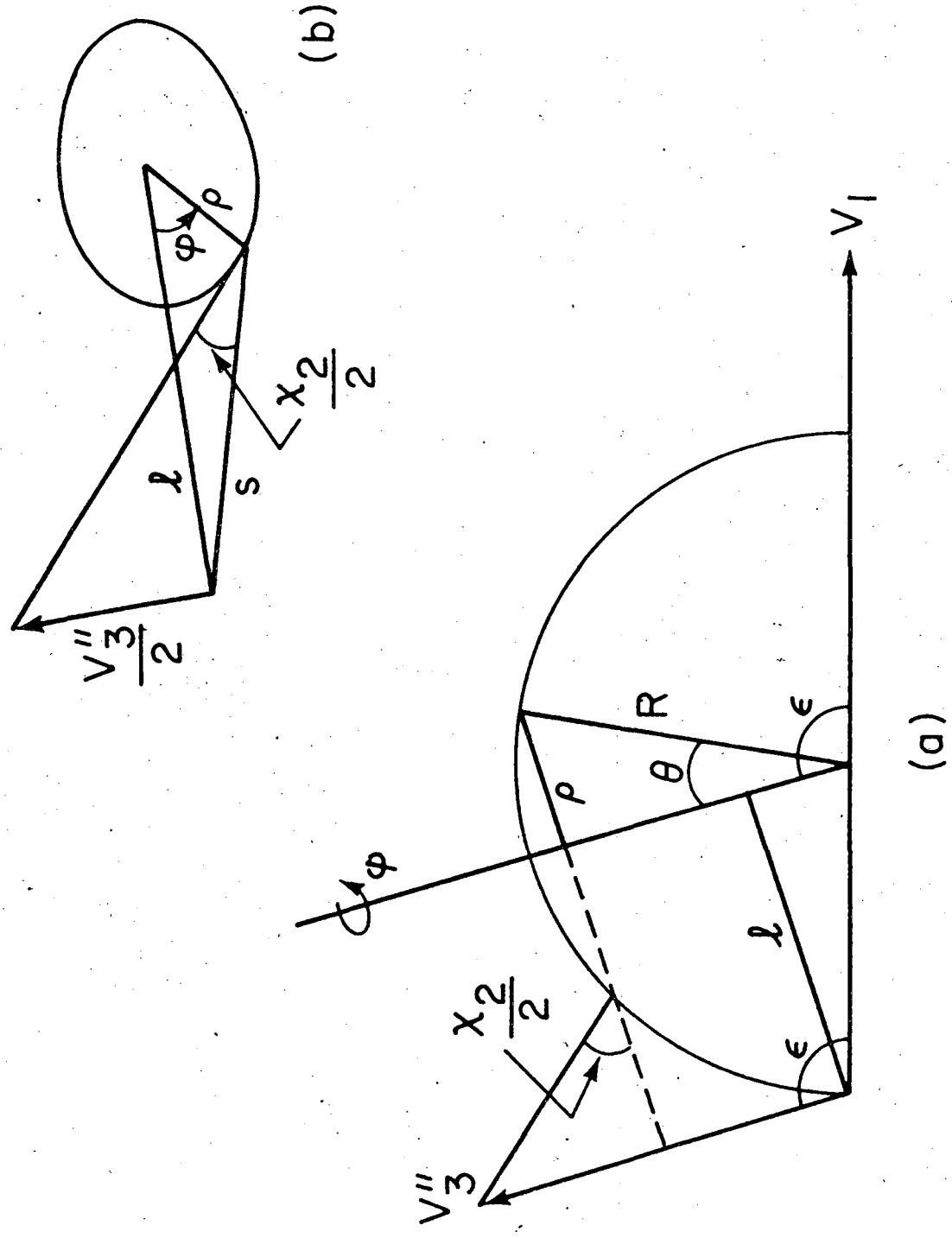

Fig. 4

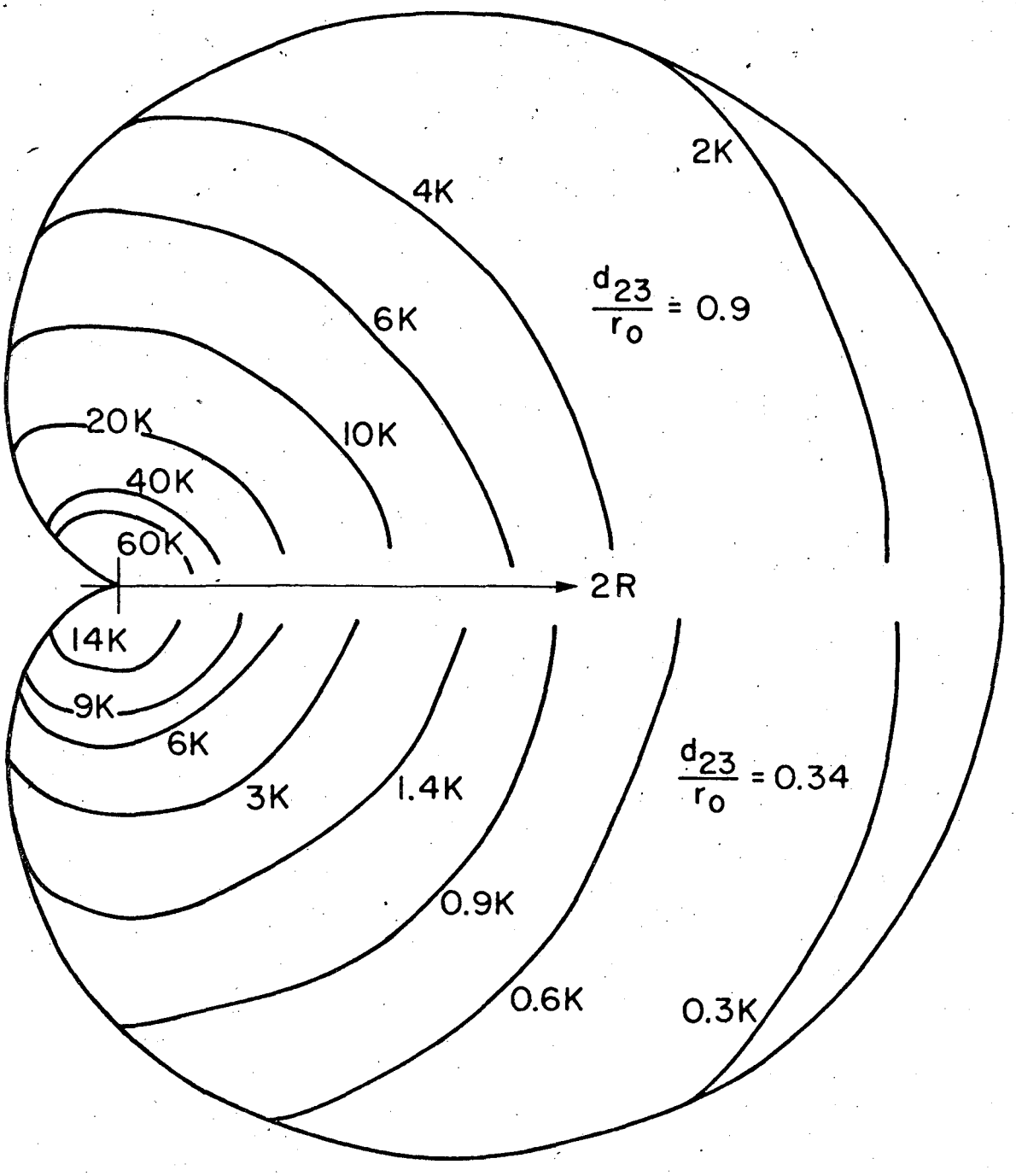

Fig. 5

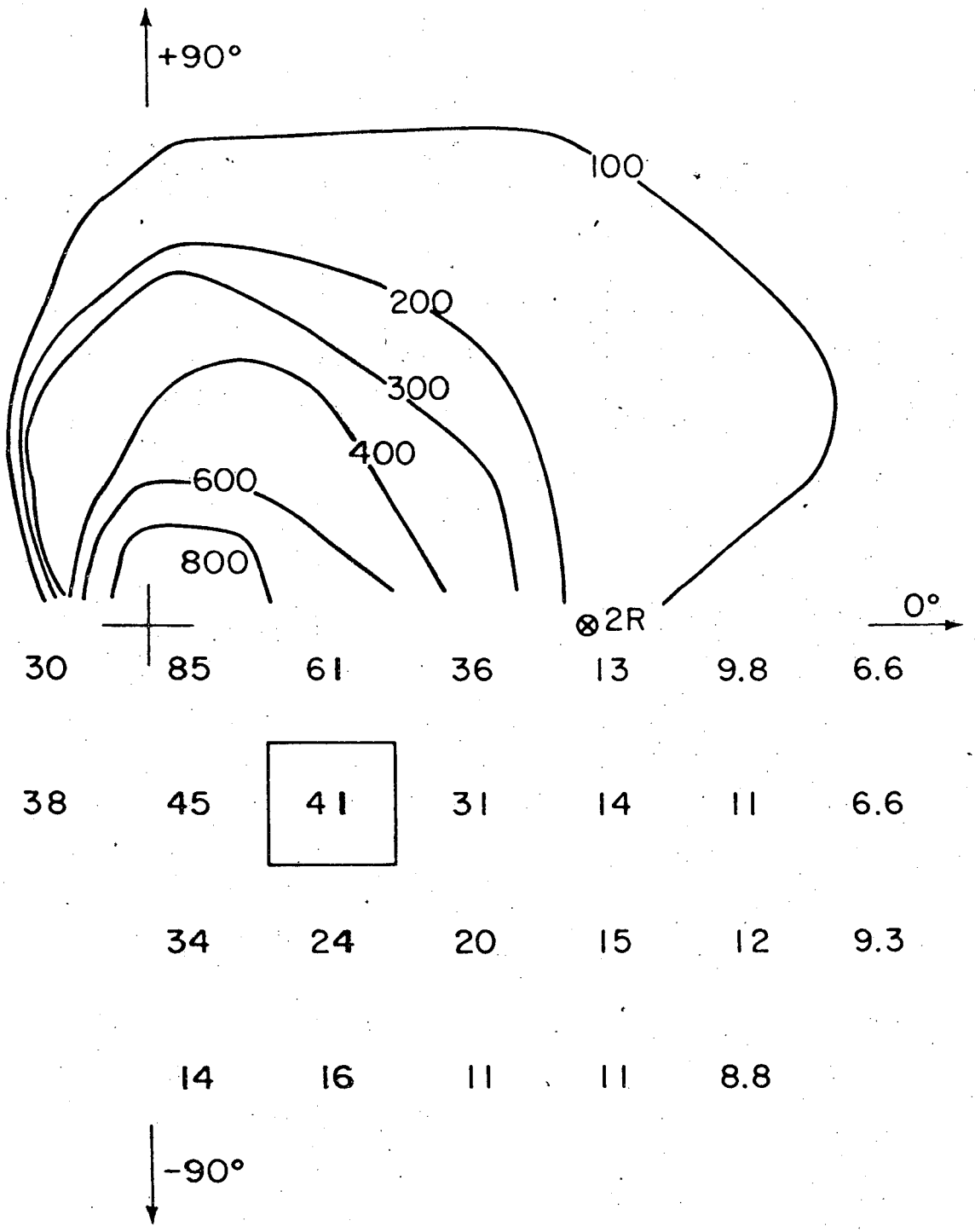
+90°
100
200
300
400
600
800
⊗2R
0°
30 85 61 36 13 9.8 6.6
38 45 41 31 14 11 6.6
34 24 20 15 12 9.3
14 16 11 11 8.8
-90°

Fig. 6

TECHNICAL INFORMATION DIVISION
LAWRENCE BERKELEY LABORATORY
UNIVERSITY OF CALIFORNIA
BERKELEY, CALIFORNIA 94720